Chemical Science

ROYAL SOCIETY OF CHEMISTRY

EDGE ARTICLE

View Article Online
View Journal | View Issue

Cite this: *Chem. Sci.*, 2024, **15**, 8873

All publication charges for this article have been paid for by the Royal Society of Chemistry

Received 14th February 2024
Accepted 3rd May 2024

DOI: 10.1039/d4sc01046a

rsc.li/chemical-science

Insulated π-conjugated 2,2′-bipyridine transition-metal complexes: enhanced photoproperties in luminescence and catalysis†

Tomohiro Iwai, *[a] Shinsuke Abe,[a] Shin-ya Takizawa, [a] Hiroshi Masai [ab] and Jun Terao *[a]

2,2′-Bipyridine has been identified as a privileged ligand scaffold for photofunctional transition metal complexes. We herein report on the synthesis and photoproperties of an insulated π-conjugated 2,2′-bipyridine with a linked rotaxane structure consisting of permethylated α-cyclodextrin (PM α-CD) and oligo(*p*-phenylene ethynylene). The insulated π-conjugated 2,2′-bipyridine exhibited enhanced ligand performance in the solid-state emitting biscyclometalated Ir complexes and visible-light-driven Ni catalysts owing to π-extension and remote steric effects based on the linked rotaxane structure.

Introduction

2,2′-Bipyridine ligand constructs π-conjugated systems containing metal atoms through *N*,*N*′-chelating coordination,[1] and is therefore widely used in photofunctional transition-metal complexes including luminescent materials,[2] photosensitizers,[3] and photocatalysts.[4] To effectively utilize visible light, π-extension of 2,2′-bipyridine has been adopted as a reliable method to reduce HOMO–LUMO gaps.[5] However, open metal coordination environments based on the planarity of 2,2′-bipyridine ligands facilitate intermolecular interactions, including π–π and metal–metal interactions, as well as additional ligation to coordinatively unsaturated metal centers (Fig. 1a),[6] resulting in the decreased performance of photofunctional transition-metal complexes. Spatial isolation of π-conjugated molecules based on steric protection effectively circumvents these problems.

In this context, three-dimensional insulation of π-conjugated molecules by nonconductive macrocycles is a promising strategy owing to its high degree of steric protection.[7] We previously reported on an insulated π-conjugated polymer containing 2,2′-bipyridine moieties that exhibits significant solid-state luminescence with typical metal coordination.[8,9] The sandwich-structured 2,2′-bipyridine with linked rotaxanes consisting of permethylated α-cyclodextrin (PM α-CD) and oligo(*p*-phenylene ethynylene) suppresses the interaction between π-conjugated chains while allowing metal ions to easily access the coordination site. We thus designed an insulated π-conjugated 2,2′-bipyridine **L1** with a linked rotaxane structure end-capped by pivaloyl groups as a ligand for photofunctional transition-metal complexes (Fig. 1b).[10] This paper describes the synthesis and characterization of **L1**, and its high ligand performance in solid-state emitting biscyclometalated Ir complexes and visible-light-driven Ni catalysts. Experimental and computational studies indicate that the enhanced performance is attributable to π-extension and remote steric effects resulting from the linked rotaxane structure.

Results and discussion

Synthesis of insulated π-conjugated 2,2′-bipyridine

Fig. 1c shows the density functional theory (DFT)-optimized model structure of **L1**. Two PM α-CDs are located outside the carbon–carbon triple bond directly connected to the 2,2′-bipyridine core, covering the diphenylacetylene units extensively. Therefore, a size-limited but molecular accessible space is around the coordinating N atom (*ca.* 11–12 Å).

The synthesis of **L1** is illustrated in Scheme 1. The Pd-catalyzed Sonogashira coupling reaction between the PM α-CD-tethered terminal alkyne **1** and 2-bromo-5-iodopyridine produced bis(phenylene ethynylene)-conjugated pyridine **2**. To construct the 2,2′-bipyridine structure, sequential stannylation and Stille coupling of **2** were conducted using Bu_3Sn–$SnBu_3$ in the presence of $[Pd(PPh_3)_4]$, affording **3**. Following the reduction of the NO_2 group with $Na_2S_2O_4$, heating NH_2-substituted 2,2′-bipyridine **4** in a mixed solvent of H_2O and MeOH (1 : 1) induced the self-inclusion of phenylene ethynylene with PM α-CD driven by hydrophilic–hydrophobic interactions.[11] Subsequent pivaloyl end capping of the terminal NH_2 group in **5**

[a]*Department of Basic Science, Graduate School of Arts and Sciences, The University of Tokyo, 3-8-1, Komaba, Meguro-ku, Tokyo, 153-8902, Japan. E-mail: ciwai@g.ecc.u-tokyo.ac.jp; cterao@mail.ecc.u-tokyo.ac.jp*

[b]*PRESTO, Japan Science and Technology Agency, 4-1-8 Honcho, 332-0012 Kawaguchi, Saitama, Japan*

† Electronic supplementary information (ESI) available: Experimental procedures, compound characterizations, and computational studies. See DOI: https://doi.org/10.1039/d4sc01046a

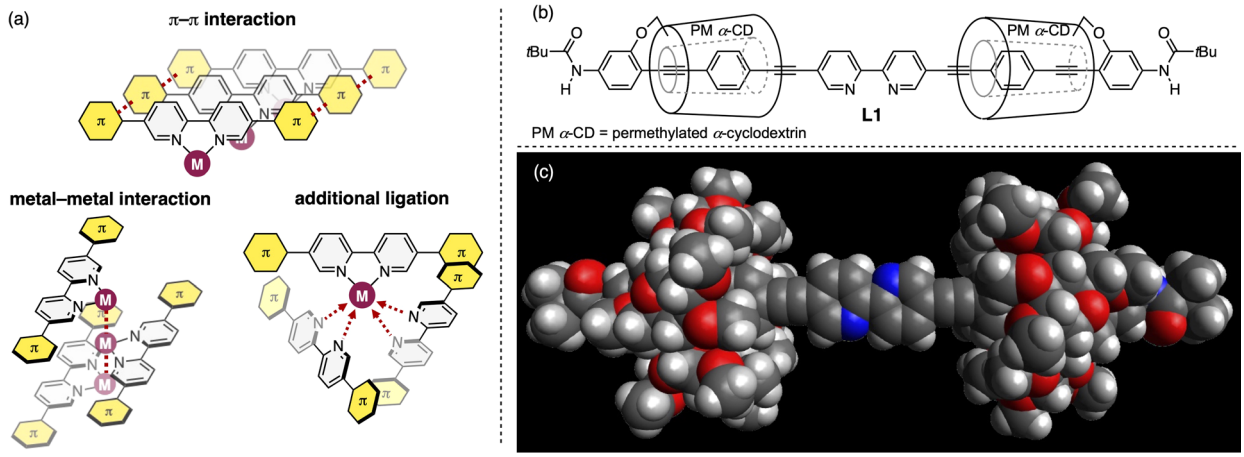

Fig. 1 (a) Conceptual diagrams illustrating issues encountered in π-extended 2,2′-bipyridine ligands. Red dotted lines show π–π and metal–metal interactions, and additional ligation to the metal center. (b) Structure of insulated π-conjugated 2,2′-bipyridine **L1** with the linked rotaxane structure end-capped by pivaloyl groups. (c) Optimized molecular structure of **L1** calculated using the B3LYP/6-31G(d,p) level.

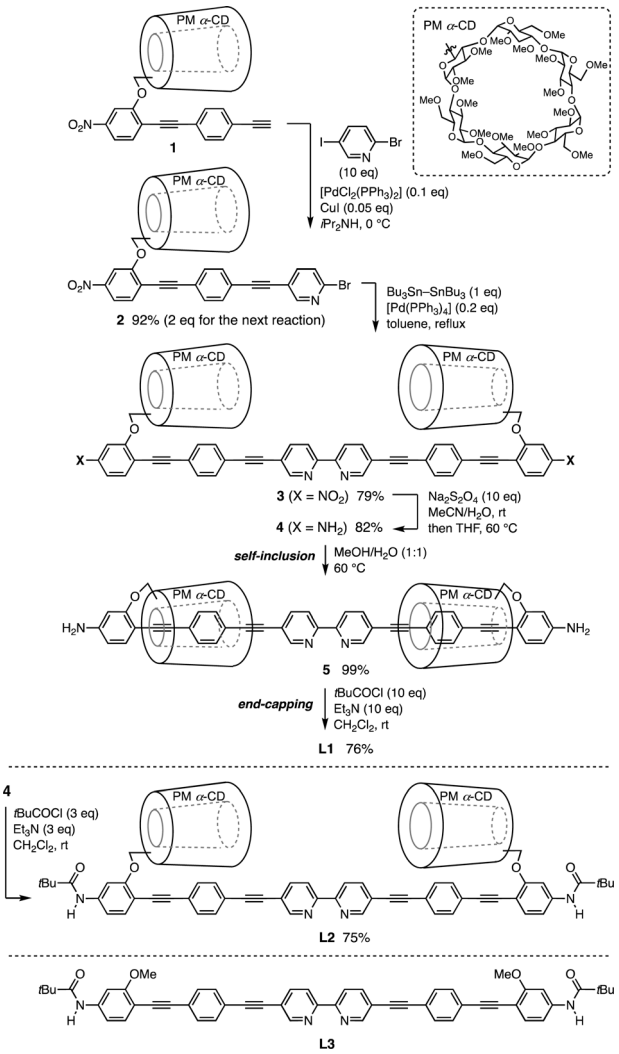

Scheme 1 Synthesis and structures of **L1**–**L3**.

furnished **L1** as an air- and moisture-stable yellow-brown solid. The insulated structure of **L1** was confirmed by the nuclear Overhauser effect (NOE) between the inner PM α-CD and phenylene protons in ^{1}H–^{1}H ROESY NMR spectra.[12] The steric hindrance of the pivaloyl group inhibits PM α-CD dethreading on nonpolar solvents, such as CH_2Cl_2 and toluene, favoring the uninsulated structure. **L2** prepared from **4** *via* direct pivaloylation in CH_2Cl_2 and **L3** with PM α-CDs removed served as uncovered references.

Luminescent biscyclometalated Ir complexes

Our previous studies on the utility of linked rotaxane structures in luminescent materials[9a,c,d,e] prompted us to apply **L1** to phosphorescent biscyclometalated Ir complexes.[13] The newly synthesized Ir complex $[Ir(ppy)_2(\mathbf{L1})]PF_6$ (ppy = 2-phenylpyridine, Fig. 2a) exhibits significant red-shift of absorption and emission peaks compared to the parent complex $[Ir(ppy)_2(bpy)]PF_6$ (bpy = 2,2′-bipyridine) (Fig. 2b and c), similar to uncovered π-extended biscyclometalated Ir complexes reported by Tatay[14a] and Schanze.[14b] Notably, unlike its uncovered counterpart $[Ir(ppy)_2(\mathbf{L3})]PF_6$, $[Ir(ppy)_2(\mathbf{L1})]PF_6$ demonstrated a higher emission quantum yield (QY) in the solid state than in the solution state (Fig. 2d). The linked rotaxane structure effectively suppresses intermolecular π–π interactions, even in the solid state where molecular aggregation is prominent (Fig. 2e). Time-dependent density functional theory (TD-DFT) calculations of $[Ir(ppy)_2(\mathbf{L3})]^+$ showed that the electronic transitions of $[Ir(ppy)_2(\mathbf{L1})]PF_6$ around 413 nm have an intraligand charge transfer (ILCT) character from the phenylene-ethynylenes to the 2,2′-bipyridine moiety, mixed with some metal-to-ligand charge transfer (MLCT) character from the Ir(III) center to the 2,2′-bipyridine moiety and ligand-to-ligand charge transfer (LLCT) character from the ppy ligand to the 2,2′-bipyridine moiety (Fig. 2f).[14–17]

Visible-light-driven Ni catalysts

The preferred ILCT nature of the excited Ir-**L1** system prompted us to investigate the applicability of **L1** as a ligand for visible-

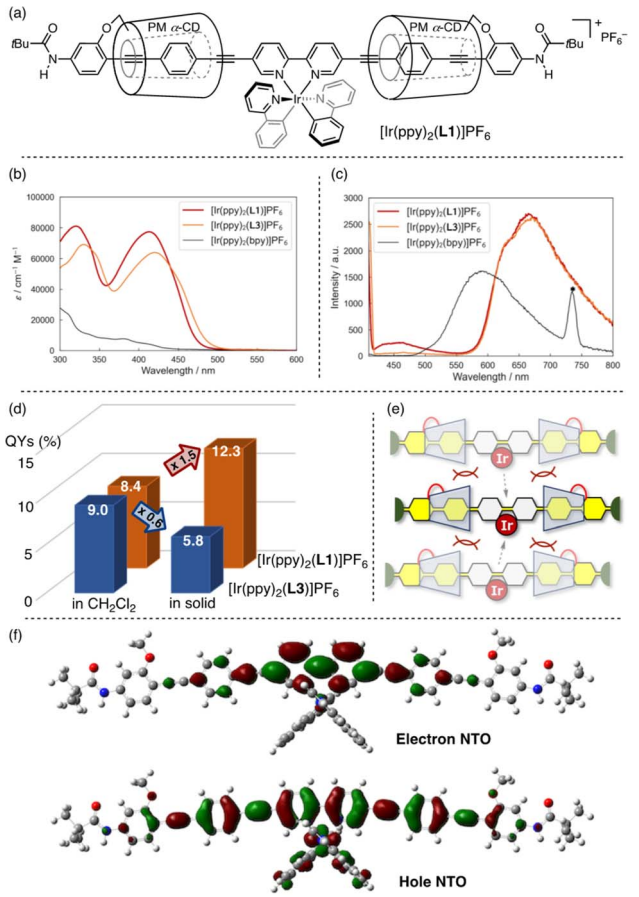

Fig. 2 (a) Molecular structure of $[Ir(ppy)_2(\mathbf{L1})]PF_6$. (b) Absorption spectra of $[Ir(ppy)_2(\mathbf{L1})]PF_6$, $[Ir(ppy)_2(\mathbf{L3})]PF_6$, and $[Ir(ppy)_2(bpy)]PF_6$ (in CH_2Cl_2, 1×10^{-5} M). (c) Emission spectra of $[Ir(ppy)_2(\mathbf{L1})]PF_6$, $[Ir(ppy)_2(\mathbf{L3})]PF_6$, and $[Ir(ppy)_2(bpy)]PF_6$ (in CH_2Cl_2, 1×10^{-6} M, under a N_2 atmosphere, excited at 405, 405, 365 nm, respectively). The asterisk indicates the second order of excitation wavelength. (d) Solution (1×10^{-6} M in CH_2Cl_2) and solid-state luminescence quantum yields (QYs) of $[Ir(ppy)_2(\mathbf{L1})]PF_6$ and $[Ir(ppy)_2(\mathbf{L3})]PF_6$ (excited at 405 nm under a N_2 atmosphere). (e) Schematic of the aggregation suppression of $[Ir(ppy)_2(\mathbf{L1})]PF_6$. (f) Natural transition orbitals (NTOs) of $[Ir(ppy)_2(\mathbf{L3})]^+$ calculated using the CAM-B3LYP/6-31+G(d,p) (for C, H, N, O) and LANL2DZ (for Ir) levels with the PCM (CH_2Cl_2) solvation model.

light-driven Ni-catalyzed cross-coupling reactions,[18] classified as metallaphotoredox catalysis,[19] merging transition metal catalysis with photocatalysis. Pieber *et al.* proposed ILCT-induced Ni-catalyzed carbon-heteroatom coupling using π-extended 2,2′-bipyridine sandwiched between two *N*-carbazolyl groups,[20] generating catalytically active Ni(I) species through single-electron reduction of bench-stable Ni(II)-bipyridine complexes under visible-light irradiation without exogenous photocatalysts.[21–23] Li *et al.* reported similar photocatalyst-free metallaphotoredox systems based on 2-(pyridin-2-yl)quinoline-based *N*,*N*′-chelating ligands.[24]

TD-DFT calculations of the model Ni complex $NiCl_2(\mathbf{L3})$ with an uncovered phenylene-ethynylene structure show that the 375 nm band (onset *ca.* 450 nm) obtained in the experimental spectrum of the Ni(II)-**L1** complex *in situ* prepared from $NiCl_2 \cdot$DME (DME: 1,2-dimethoxyethane) and **L1** in DMF (*N*,*N*-dimethylformamide) is attributed to ILCT transitions from the phenylene-ethynylene to 2,2′-bipyridine moieties (Fig. 3a). The natural transition orbital (NTO) distribution of $NiCl_2(\mathbf{L3})$ was similar to that of the carbazole-bipyridine Ni(II) complex reported by Pieber *et al.* (Fig. 3b),[20] implying that Ni(I) species could be formed from the Ni(II)-**L1** system *via* ILCT transitions during the catalytic reaction.

The Ni(II)-**L1** system was prepared *in situ* from $NiCl_2 \cdot$DME (1 mol%) and **L1** (1 mol%), and applied to the C–O coupling of 4-bromobenzonitrile (**6a**, 0.1 mmol) and MeOH (4 mmol) in DMF (0.2 M) under 427 nm LED irradiation for 20 h in the presence of $i\mathrm{Pr}_2\mathrm{EtN}$ as a base with cooling fans.[18c] To our delight, the reaction proceeded smoothly without the use of an exogenous photocatalyst, yielding 94% of 4-methoxybenzonitrile **7a** (Table 1, entry 1). In contrast, no reaction was observed in the dark (entry 2). The reaction did not proceed without the nickel salt or **L1** (entries 3 and 4). Using the simple parent 2,2′-bipyridine instead of **L1** produced no reaction (entry 5). Therefore, a combination of the nickel salt, **L1**, and visible light irradiation is required.

In contrast to the results obtained using **L1**, the uncovered counterparts **L2** and **L3** were less effective (27 and 0%, entries 6 and 7). This suggests that the steric effects of the linked rotaxane structure in **L1** are critical. Furthermore, increasing **L1** loading from 1 mol% (94%, entry 1) to 2 mol% (84%, entry 8) did not significantly reduce reaction efficiency, whereas using 2 mol% **L2** resulted in almost loss of activity (8%, entry 9). Based on the optimal structure of **L1** (Fig. 1c), we postulated that the linked rotaxane structure, with fixed PM α-CD positions, induced a remote steric effect that inhibited the coordination of the secondary ligand molecules to the catalytically active

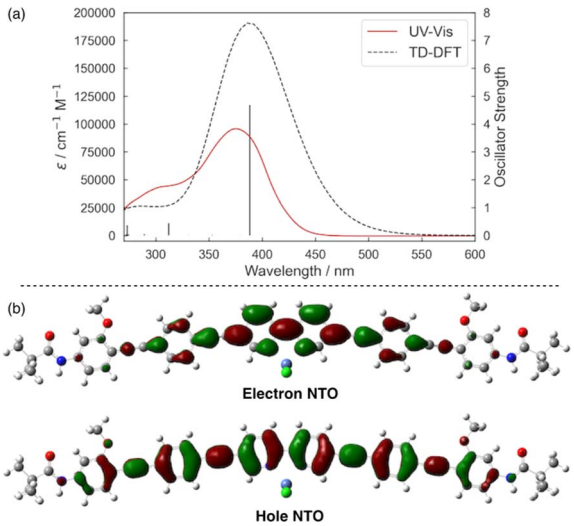

Fig. 3 (a) Experimental (red solid line) and calculated (black dashed line) UV/Visible spectra of $NiCl_2 \cdot$DME/**L1** (1 : 1, in DMF) and $NiCl_2(\mathbf{L3})$, respectively. A vertical line is assigned to an intraligand charge transfer (ILCT) transition. (b) NTOs of $NiCl_2(\mathbf{L3})$ calculated using the CAM-UB3LYP/6-31+G(d,p) (for C, H, N, O, Cl) and LANL2DZ (for Ni) levels with the PCM (DMF) solvation model.

Table 1 Visible-light-driven Ni-catalyzed C–O coupling between **6a** and MeOH[a]

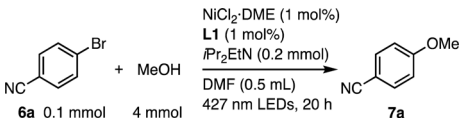

Entry	Variation	Conv. of **6a**[b] (%)	Yield of **7a**[b] (%)
1	None	97	94 (68)
2	No light	0	0
3	No $NiCl_2 \cdot DME$	0	0
4	No **L1**	0	0
5	bpy instead of **L1**	1	0
6	**L2** instead of **L1**	29	27
7	**L3** instead of **L1**	1	0
8	**L1** (2 mol%)	86	84
9	**L2** (2 mol%) instead of **L1**	10	8

[a] Conditions: 4-bromobenzonitrile (**6a**, 0.1 mmol), MeOH (4 mmol), $NiCl_2 \cdot DME$ (1 mol%), **L1** (1 mol%), iPr_2EtN (0.2 mmol), DMF (0.5 mL), 1,3,5-trimethoxybenzene (0.1 mmol) as an internal standard, 427 nm LEDs, 20 h, with cooling fans. [b] Determined by ^1H NMR using an internal standard. The isolated yields are shown in parentheses.

monochelating Ni species. This assumption is supported by our previous discovery of the mono-chelating properties of dumbbell-shaped 2,2′-bipyridines with triarylmethyl substituents at the C5 and C5′ positions.[25]

The Ni(II)-**L1** system enabled efficient C–O coupling of several aryl halides and alcohols (Scheme 2). An electro-deficient aryl bromide, methyl 4-bromobenzoate, was an appropriate substrate, yielding **7b** in 73% isolated yield. Although the reaction of 4-bromoanisole, which was electronically deactivated by the MeO group, was less effective, the use of the corresponding aryl iodide, 4-iodoanisole, with increasing the amount of MeOH and extending the reaction time (80 equiv., 48 h), allowed the coupling to produce **7c** in 60% yield. The use of *n*-hexanol as the nucleophile also resulted in the complete consumption of **6a**, yielding **7d** in a reasonable yield with minor formation of the hydration product 4-hydroxybenzonitrile (**7f**, 28%). A secondary alcohol, cyclopentanol, was coupled with 4-iodobenzonitrile under the modified conditions (80 equiv, 48 h), yielding **7e** in 50% yield.

H_2O also contributes to C–O coupling at low catalyst loadings (Scheme 2). The reaction between **6a** and H_2O proceeded smoothly with the 0.1 mol% Ni-**L1** catalyst, yielding **7f** in 88% isolated yield. The 10 mmol-scale reaction of **6a** with the 0.02 mol% Ni loading afforded **7f** in 66% yield, corresponding to the turnover number (TON) of 3300. The reaction efficacy with **L1** was comparable to those with other state-of-art visible-light-driven Ni catalysts.[23,26] An *ortho*-substituted aryl bromide, 2-bromobenzonitrile, also reacted with H_2O in the presence of 0.2 mol% Ni loading, yielding **7g** in 75% yield, and a minor formation of the homocoupling product [1,1′-biphenyl]-2,2′-dicarbonitrile (24%).

Furthermore, **L1** was applicable to Ni-catalyzed C–N coupling under visible light irradiation (Scheme 3).[18b,27] With **L1**, the

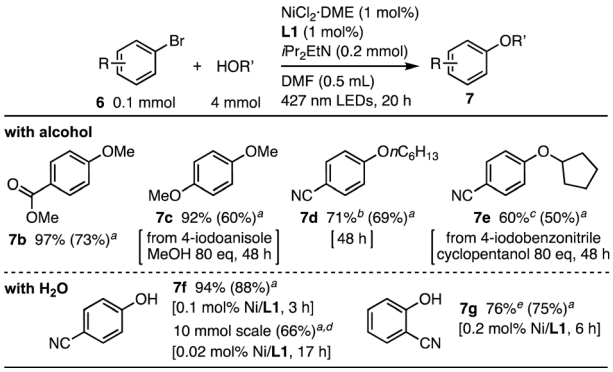

Scheme 2 Substrate scope in the visible-light-driven Ni-catalyzed C–O coupling with **L1**. Conditions: aryl bromide (**6**, 0.1 mmol), HOR′ (4 mmol), $NiCl_2 \cdot DME$ (1 mol%), **L1** (1 mol%), iPr_2EtN (0.2 mmol), DMF (0.5 mL), 1,3,5-trimethoxybenzene as an internal standard (0.1 mmol), 427 nm LEDs, 20 h with cooling fans. Determined by ^1H NMR analysis using an internal standard. [a] Isolated yields. [b] Hydration product **7f** was also obtained in 28% NMR yield. [c] Some unreacted 4-iodobenzonitrile remained in the crude product (83% conversion). Dehaloprotonation product, benzonitrile, was also obtained in 20% NMR yield. [d] **6a** (10 mmol), H_2O (40 mmol), $NiCl_2 \cdot DME$ (0.02 mol%), **L1** (0.02 mol%), iPr_2EtN (20 mmol), DMF (7.5 mL), 427 nm LEDs, 17 h with cooling fans. Complete conversion of **6a** was observed. The dehaloprotonation product, benzonitrile, was also formed. [e] The homocoupling product, [1,1′-biphenyl]-2,2′-dicarbonitrile, was also obtained in 24% NMR yield.

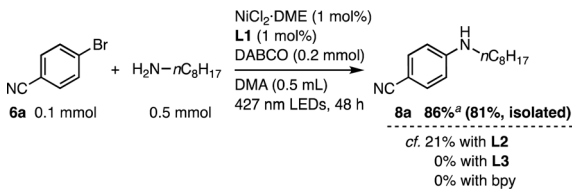

Scheme 3 Visible-light-driven Ni-catalyzed C–N coupling. Conditions: 4-bromobenzonitrile (**6a**, 0.1 mmol), H_2N-nC_8H_{17} (0.5 mmol), $NiCl_2 \cdot DME$ (1 mol%), **L1** (1 mol%), DABCO (0.2 mmol), DMA (0.5 mL), 1,3,5-trimethoxybenzene as an internal standard (0.1 mmol), 427 nm LEDs, 48 h with cooling fans. Determined by ^1H NMR analysis using an internal standard. Isolated yields are shown in parentheses. [a] Hydration product **7f** was also obtained in 13% NMR yield.

reaction between **6a** and *n*-octylamine was successful with 1 mol% Ni loading in the presence of 1,4-diazabicyclo[2.2.2]octane (DABCO) as the base in *N*,*N*-dimethylacetamide (DMA) under 427 nm LED irradiation, yielding **8a** in 86% NMR yield and a small amount of hydration product **7f** (13%). In contrast, the use of **L2**, **L3**, or 2,2′-bipyridine resulted in lower efficiency, with either no reaction or only a low conversion reaction occurring, emphasizing the importance of the linked rotaxane structure.

Conclusion

The insulated π-conjugated 2,2′-bipyridine **L1** bearing a linked rotaxane structure consisting of PM α-CDs and *p*-phenylene ethynylenes at the C5 and C5′ positions was synthesized. **L1** outperformed uncovered 2,2′-bipyridine ligands in the solid-

state emitting biscyclometalated Ir complex and visible-light-driven Ni-catalyzed C–O and C–N coupling without exogenous photocatalysts owing to the π-extension and remote steric effects based on the linked rotaxane structure. The validity of ILCT processes from phenylene-ethynylene to 2,2′-bipyridine moieties *via* photoexcitation was demonstrated *via* TD-DFT calculations. This study provides new design guidelines for photofunctional transition-metal complexes and contributes to further development in the field of luminescent materials and synthetic catalysis. Further investigation of applications of the insulated π-conjugated 2,2′-bipyridines for photofunctional transition-metal complexes is ongoing in our laboratory.

Data availability

All experimental procedures and spectroscopic data can be found in the ESI.†

Author contributions

T. I. and J. T. conceived and supervised the idea. S. A. performed all experiments. All authors discussed the results and wrote the manuscript.

Conflicts of interest

The authors declare no conflict of interest.

Acknowledgements

This research was partially supported by JSPS KAKENHI Grant Number JP22K19022 (T. I.), JP22H02060 (J. T.), by JST CERST Grant Number JPMJCR19I2 (J. T.), by NEDO Grant Number JPNP21016 (J. T.), by Toshiaki Ogasawara Memorial Foundation (J. T.), and by The Yamada Science Foundation (J. T.). We thank Dr Hiromichi V. Miyagishi (Hokkaido University) for fruitful discussion on the early work.

Notes and references

1 For selected reviews on 2,2′-bipyridine, see: (*a*) C. Kaes, A. Katz and M. W. Hosseini, *Chem. Rev.*, 2000, **10**, 3553–3590; (*b*) E. C. Constable and C. E. Housecroft, *Molecules*, 2019, **24**, 3951.

2 M. D. Ward, C. M. White, F. Barigelletti, N. Armaroli, G. Calogero and L. Flamigni, *Coord. Chem. Rev.*, 1998, **171**, 481–488.

3 (*a*) M. A. Munegowda, A. Manalac, M. Weersink, S. A. McFarland and L. Lilge, *Coord. Chem. Rev.*, 2022, **470**, 214712; (*b*) T. S. Teets and Y. Wu, Organometallic Photosensitizers, *In Comprehensive Organometallic Chemistry IV*, ed. G. Parkin, K. Meyer and D. O'hare, Elsevier, Oxford, UK, 2022, pp. 284–338.

4 K. Teegardin, J. I. Day, J. Chan and J. Weaver, *Org. Process Res. Dev.*, 2016, **20**, 1156–1163.

5 H. S. Joshi, R. Jamshidi and Y. Tor, *Angew. Chem., Int. Ed.*, 1999, **38**, 2721–2725.

6 (*a*) H. L.-K. Fu, C. Po, H. He, S. Y.-L. Leung, K. S. Wong and V. W.-W. Yam, *Chem.–Eur. J.*, 2016, **22**, 11826–11836; (*b*) P. V. Petrović, G. V. Janjić and S. D. Zarić, *Cryst. Growth Des.*, 2014, **14**, 3880–3889; (*c*) R. Palmans, D. B. MacQueen, C. G. Pierpont and A. J. Frank, *J. Am. Chem. Soc.*, 1996, **118**, 12647–12653.

7 (*a*) M. J. Frampton and H. L. Anderson, *Angew. Chem., Int. Ed.*, 2007, **46**, 1028–1064; (*b*) H. Masai and J. Terao, *Bull. Chem. Soc. Jpn.*, 2019, **92**, 529–539; (*c*) C. Pan, C. Zhao, M. Takeuchi and K. Sugiyasu, *Chem.–Asian J.*, 2015, **10**, 1820–1835.

8 T. Hosomi, H. Masai, T. Fujihara, Y. Tsuji and J. Terao, *Angew. Chem., Int. Ed.*, 2016, **55**, 13427–13431.

9 For selected examples on the linked rotaxane-base materials reported by our groups, see: (*a*) T. Kaneko, G. M. Russell, Y. Kawano, H. Masai and J. Terao, *Angew. Chem., Int. Ed.*, 2023, **62**, e202305374; (*b*) S.-Y. Chou, H. Masai, M. Otani, H. V. Miyagishi, G. Sakamoto, Y. Yamada, Y. Kinoshita, H. Tamiaki, T. Katase, H. Ohta, T. Kondo, A. Nakada, R. Abe, T. Tanaka, K. Uchida and J. Terao, *Appl. Catal., B*, 2023, **327**, 122373; (*c*) G. M. Russell, T. Kaneko, S. Ishino, H. Masai and J. Terao, *Adv. Funct. Mater.*, 2022, **32**, 2205855; (*d*) H. Masai, T. Yokoyama, H. V. Miyagishi, M. Liu, Y. Tachibana, T. Fujihara, Y. Tsuji and J. Terao, *Nat. Commun.*, 2020, **11**, 408; (*e*) H. Masai, J. Terao, S. Makuta, Y. Tachibana, T. Fujihara and Y. Tsuji, *J. Am. Chem. Soc.*, 2014, **136**, 14714–14717; (*f*) H. Masai, J. Terao, S. Seki, S. Nakashima, M. Kiguchi, K. Okoshi, T. Fujihara and Y. Tsuji, *J. Am. Chem. Soc.*, 2014, **136**, 1742–1745; (*g*) J. Terao, A. Wadahama, A. Matono, T. Tada, S. Watanabe, S. Seki, T. Fujihara and Y. Tsuji, *Nat. Commun.*, 2013, **4**, 1691; (*h*) J. Terao, Y. Tanaka, S. Tsuda, N. Kambe, M. Taniguchi, T. Kawai, A. Saeki and S. Seki, *J. Am. Chem. Soc.*, 2009, **131**, 18046–18047; (*i*) J. Terao, S. Tsuda, Y. Tanaka, K. Okoshi, T. Fujihara, Y. Tsuji and N. Kambe, *J. Am. Chem. Soc.*, 2009, **131**, 16004–16005.

10 For selected examples on cyclodextrin-based ligands on metal complexes, see: (*a*) T.-A. Phan, N. Armaroli, A. S. Moncada, E. Bandini, B. Delavaux-Nicot, J.-F. Nierengarten and D. Armspach, *Angew. Chem., Int. Ed.*, 2023, **62**, e202214638; (*b*) G. Xu, S. Leloux, P. Zhang, J. M. Suárez, Y. Zhang, E. Derat, M. Ménand, O. Bistri-Aslanoff, S. Roland, T. Leyssens, O. Riant and M. Sollogoub, *Angew. Chem., Int. Ed.*, 2020, **59**, 7591–7597; (*c*) H. Kitagishi, D. Shimoji, T. Ohta, R. Kamiya, Y. Kudo, A. Onoda, T. Hayashi, J. Weiss, J. A. Wytko and K. Kano, *Chem. Sci.*, 2018, **9**, 1989–1995; (*d*) P. Zhang, C. Tugny, J. M. Suárez, M. Guitet, E. Derat, N. Vanthuyne, Y. Zhang, O. Bistri, V. Mouriès-Mansuy, M. Ménand, S. Roland, L. Fensterbank and M. Sollogoub, *Chem*, 2017, **3**, 174–191; (*e*) M. Jouffroy, D. Armspach, D. Matt, K. Osakada and D. Takeuchi, *Angew. Chem., Int. Ed.*, 2016, **55**, 8367–8370; (*f*) M. Jouffroy, R. Gramage-Doria, D. Armspach, D. Sémeril, W. Oberhauser, D. Matt and L. Toupet, *Angew. Chem., Int. Ed.*, 2014, **53**, 3937–3940; (*g*) M. Guitet, P. Zhang, F. Marcelo, C. Tugny, J. Jiménez-Barbero, O. Buriez, C. Amatore, V. Mouriès-Mansuy, J.-P. Goddard,

L. Fensterbank, Y. Zhang, S. Roland, M. Ménand and M. Sollogoub, *Angew. Chem., Int. Ed.*, 2013, **52**, 7213–7218, for a related review, see: (*h*) D. Armspach and D. Matt, *C. R. Chim.*, 2011, **14**, 135–148.

11 (*a*) H. Masai, J. Terao, T. Fujihara and Y. Tsuji, *Chem.–Eur. J.*, 2016, **22**, 6624–6630; (*b*) R. Nishiyabu and K. Kano, *Eur. J. Org Chem.*, 2004, **2004**, 4985–4988.

12 (*a*) S. Menuel, N. Azaroual, D. Landy, N. Six, F. Hapiot and E. Monflier, *Chem.–Eur. J.*, 2011, **17**, 3949–3955; (*b*) T. Fujimoto, Y. Sakata and T. Kaneda, *Chem. Commun.*, 2000, 2143–2144.

13 For selected reviews on cyclometalated Ir(III) complexes, see: (*a*) H. Shi, Y. Wang, S. Lin, J. Lou and Q. Zhang, *Dalton Trans.*, 2021, **50**, 6410–6417; (*b*) C. Caporale and M. Massi, *Coord. Chem. Rev.*, 2018, **363**, 71–91; (*c*) R. D. Costa, E. Ortí, H. J. Bolink, F. Monti, G. Accorsi and N. Armaroli, *Angew. Chem., Int. Ed.*, 2012, **51**, 8178–8211; (*d*) Y. Chi and P.-T. Chou, *Chem. Soc. Rev.*, 2010, **39**, 638–655; (*e*) L. Flamigni, A. Barbieri, C. Sabatini, B. Ventura and F. Barigelletti, *Top. Curr. Chem.*, 2007, **281**, 143–203; (*f*) M. S. Lowry and S. Bernhard, *Chem.–Eur. J.*, 2006, **12**, 7970–7977.

14 For cyclometalated Ir(III) complexes with diimine ligands bearing phenylene-ethynylenes, see: (*a*) J. Ponce, J. Aragó, I. Vayá, J. G. Magenti, S. Tatay, E. Ortí and E. Coronado, *Eur. J. Inorg. Chem.*, 2016, 1851–1859; (*b*) K. D. Glusac, S. Jiang and K. S. Schanze, *Chem. Commun.*, 2002, 2504–2505.

15 For selected examples of luminescence transition metal complexes with π-extended diimine ligands, see: (*a*) J. M. Van Raden, S. Louie, L. N. Zakharov and R. Jasti, *J. Am. Chem. Soc.*, 2017, **139**, 2936–2939; (*b*) N. Zhao, Y.-H. Wu, H.-M. Wen, X. Zhang and Z.-N. Chen, *Organometallics*, 2009, **28**, 5603–5611; (*c*) Q. Zhao, S. Liu, M. Shi, C. Wang, M. Yu, L. Li, F. Li, T. Yi and C. Huang, *Inorg. Chem.*, 2006, **45**, 6152–6160; (*d*) A. Kokil, P. Yao and C. Weder, *Macromolecules*, 2005, **38**, 3800–3807; (*e*) K. A. Walters, K. D. Ley, C. S. P. Cavalaheiro, S. E. Miller, D. Gosztola, M. R. Wasielewski, A. P. Bussandri, H. van Willigen and K. S. Schanze, *J. Am. Chem. Soc.*, 2001, **123**, 8329–8342; (*f*) T. Pautzsch, C. Rode, E. Klemm and J. Prakt, *Chem*, 1999, **341**, 548–551; (*g*) K. D. Ley, C. E. Whittle, M. D. Bartberger and K. S. Schanze, *J. Am. Chem. Soc.*, 1997, **119**, 3423–3424; (*h*) Z. Peng, A. R. Gharavi and L. Yu, *J. Am. Chem. Soc.*, 1997, **119**, 4622–4632, for a related review, see: (*i*) Y. Liu, Y. Li and K. S. Schanze, *J. Photochem. Photobiol., C*, 2002, **3**, 1–23.

16 See the ESI† for TD-DFT calculations of $[Ir(ppy)_2(\mathbf{L3})]^+$ (Tables S2, S3 and Fig. S43†).

17 Emission quantum yields of $[Ir(ppy)_2(bpy)]PF_6$ in the solution (in CH_2Cl_2, 1×10^{-5} M) and solid states were 31.6 and 19.0% (excited at 365 nm under N_2 atmosphere), respectively. See the ESI† for absorption-emission spectra of all biscyclometalated Ir(III) complexes in solution and solid states (Fig. S45–S47†).

18 For seminal papers on dual Ni/photoredox catalyzed cross-coupling, see: (*a*) E. R. Welin, C. Le, D. M. Arias-Rotondo, J. K. McCusker and D. W. C. MacMillan, *Science*, 2017, **355**, 380–385; (*b*) E. B. Corcoran, M. T. Pirnot, S. Lin, S. D. Dreher, D. A. DiRocco, I. W. Davies, S. L. Buchwald and D. W. C. MacMillan, *Science*, 2016, **353**, 279–283; (*c*) J. A. Terrett, J. D. Cuthbertson, V. W. Shurtleff and D. W. C. MacMillan, *Nature*, 2015, **524**, 330–334; (*d*) Z. Zuo, D. T. Ahneman, L. Chu, J. A. Terrett, A. G. Doyle and D. W. C. MacMillan, *Science*, 2014, **345**, 437–440; (*e*) J. C. Tellis, D. N. Primer and G. A. Molander, *Science*, 2014, **345**, 433–436.

19 For selected reviews on metallaphotoredox catalysis, see: (*a*) A. Y. Chan, I. B. Perry, N. B. Bissonnette, B. F. Buksh, G. A. Edwards, L. I. Frye, O. L. Garry, M. N. Lavagnino, B. X. Li, Y. Liang, E. Mao, A. Millet, J. V. Oakley, N. L. Reed, H. A. Sakai, C. P. Seath and D. W. C. MacMillan, *Chem. Rev.*, 2022, **122**, 1485–1542; (*b*) S. K. Kariofillis and A. G. Doyle, *Acc. Chem. Res.*, 2021, **54**, 988–1000; (*c*) C. Zhu, H. Yue, L. Chu and M. Rueping, *Chem. Sci.*, 2020, **11**, 4051–4064; (*d*) J. Twilton, C. Le, P. Zhang, M. H. Shaw, R. W. Evans and D. W. C. MacMilan, *Nat. Rev. Chem*, 2017, **1**, 0052; (*e*) L. N. Cavalcanti and G. A. Molander, *Top. Curr. Chem.*, 2016, **374**, 39.

20 C. Cavedon, S. Gisbertz, S. Reischauer, S. Vogl, E. Sperlich, J. H. Burke, R. F. Wallick, S. Schrottke, W.-H. Hsu, L. Anghileri, Y. Pfeifer, N. Richter, C. Teutloff, H. Müller-Werkmeister, D. Cambié, P. H. Seeberger, J. Vura-Weis, R. M. van der Veen, A. Thomas and B. Pieber, *Angew. Chem., Int. Ed.*, 2022, **61**, e202211433.

21 For selected papers on studies of Ni(I) species in Ni-catalyzed cross-coupling reactions, see: (*a*) N. A. Till, S. Oh, D. W. C. MacMillan and M. J. Bird, *J. Am. Chem. Soc.*, 2021, **143**, 9332–9337; (*b*) N. A. Till, L. Tian, Z. Dong, G. D. Scholes and D. W. C. MacMillan, *J. Am. Chem. Soc.*, 2020, **142**, 15830–15841; (*c*) R. Sui, Y. Qin and D. G. Nocera, *Angew. Chem., Int. Ed.*, 2020, **59**, 9527–9533; (*d*) S. I. Ting, S. Garakyaraghi, C. M. Taliaferro, B. J. Shields, G. D. Scholes, F. N. Castellano and A. G. Doyle, *J. Am. Chem. Soc.*, 2020, **142**, 5800–5810; (*e*) R. Sun, Y. Qin, S. Ruccolo, C. Schnedermann, C. Costentin and D. G. Nocera, *J. Am. Chem. Soc.*, 2019, **141**, 89–93; (*f*) B. J. Shields, B. Kudisch, G. D. Scholes and A. G. Doyle, *J. Am. Chem. Soc.*, 2018, **140**, 3035–3039.

22 Recently, photocatalyst-free, light-induced Ni-catalyzed cross-coupling reactions with or without simple 2,2′-bipyridine-based ligands have been reported. For selected examples, see: (*a*) H. Luo, G. Wang, Y. Feng, W. Zheng, L. Kong, Y. Ma, S. Matsunaga and L. Lin, *Chem.–Eur. J.*, 2023, **29**, e202202385; (*b*) L. Yang, H.-H. Lu, C.-H. Lai, G. Li, W. Zhang, R. Cao, F. Liu, C. Wang, J. Xiao and D. Xue, *Angew. Chem., Int. Ed.*, 2020, **59**, 12714–12719; (*c*) C.-H. Lim, M. Kudisch, B. Liu and G. M. Miyake, *J. Am. Chem. Soc.*, 2018, **140**, 7667–7673; for a related review, see: (*d*) H. Luo, Y. Feng and L. Lin, *ChemCatChem*, 2023, **15**, e202300303.

23 Recently, heterogeneous dual Ni/photoredox catalyst systems with π-conjugated covalent organic frameworks

have been reported. For selected examples, see: (*a*) Y. Fan, D. W. Kang, S. Labalme and W. Lin, *J. Am. Chem. Soc.*, 2023, **145**, 25074–25079; (*b*) Y. Fan, D. W. Kang, S. Labalme, J. Li and W. Lin, *Angew. Chem., Int. Ed.*, 2023, **62**, e202218908; (*c*) A. Jati, S. Dam, S. Kumar, K. Kumar and B. Maji, *Chem. Sci.*, 2023, **14**, 8624–8634.

24 J. Li, C.-Y. Huang and C.-J. Li, *Chem*, 2022, **8**, 2419–2431.

25 Y. Kim, T. Iwai, S. Fujii, K. Ueno and M. Sawamura, *Chem.–Eur. J.*, 2021, **27**, 2289–2293.

26 Y. Pan, N. Zhang, C.-H. Liu, S. Fan, S. Guo, Z.-M. Zhang and Y.-Y. Zhu, *ACS Catal.*, 2020, **10**, 11758–11767.

27 M. Kuai, Z. Jia, L. Chen, S. Gao and W. Fang, *Eur. J. Org Chem.*, 2024, **27**, e202300933.